Nuclear Inst. and Methods in Physics Research B 476 (2020) 44–51

Contents lists available at ScienceDirect

Nuclear Inst. and Methods in Physics Research B

journal homepage: www.elsevier.com/locate/nimb

Formation region effects in x-ray transition radiation from 1 to 6 GeV electrons in multilayer targets

S.V. Trofymenko[a,c,*], R.M. Nazhmudinov[b,d], A.V. Shchagin[a,b], A.S. Kubankin[b,d], A.P. Potylitsyn[e], A.S. Gogolev[e], N.A. Filatov[e], G. Kube[f], N.A. Potylitsina-Kube[f], M. Stanitzki[f], R. Diener[f], A. Novokshonov[f]

[a] NSC 'Kharkiv Institute of Physics and Technology', Kharkiv, Ukraine
[b] NRU 'Belgorod State University', Belgorod, Russia
[c] Karazin Kharkiv National University, Kharkiv, Ukraine
[d] Lebedev Physical Institute, Moscow, Russia
[e] Tomsk Polytechnic University, Tomsk, Russia
[f] Deutsches Elektronen-Synchrotron (DESY), Hamburg, Germany

ARTICLE INFO

Keywords:
High-energy electron beam
X-ray transition radiation
Multilayer radiator
Radiation formation length
"half-bare" electron

ABSTRACT

The formation region effects in x-ray transition radiation have been experimentally investigated. The radiation was generated using 1–6 GeV electrons impinging on two multilayer targets with considerably different periods. The absolute yield of transition radiation was measured and the wide spectral peak in the range from 10 to 30 keV was observed. In the most part of the electron energy range the emission from the short-period radiator was expectedly suppressed, compared to the case of the long-period one. But for the electron energy of 1 GeV an opposite effect, though rather small, of the emission enhancement in the short-period radiator was observed. The conditions, under which this effect is much stronger, are derived and its possible practical value is outlined. The theory accounting for an arbitrary transversal shape of the electron beam and the finite size of the detector is developed. This theory describes rather well the experimental results.

1. Introduction

Transition radiation (TR) occurs when a charged particle crosses the boundary between two media with different dielectric properties. A simplest case of this kind is the particle crossing of a thin foil situated in vacuum or gas. Such an emission develops within the spatial region known as the formation region (or length) l_F (see, e.g. [1,2]). If one neglects the influence of the polarization of the medium around the foil (e. g., for very high emitted photon energies), for relativistic particles it is possible to estimate this distance as $l_F \sim \gamma^2\lambda/\pi$, where γ is the Lorentz-factor of the incident particle and λ is the radiation wavelength. After crossing the foil, within the distance l_F, the field around the incident particle with the wavelengths larger than λ is somewhat suppressed. This means that the total field around the particle lacks a low-frequency part of Fourier components compared to the conventional Coulomb field of a relativistic charged particle. Such suppression can be considered as a destructive interference of the particle's Coulomb field with the field of TR emitted in the direction of the particle motion. A particle with such an incomplete field is sometimes called "half-bare" (the term was introduced in [3]). At high particle energies the formation length can become macroscopically large and the particle can experience further interactions within it. For instance, the particle can impinge upon the second (downstream) foil producing TR again. The properties of this radiation by the "half-bare" particle, generated within the formation region l_F, noticeably differ from the conventional properties of TR by a particle with the Coulomb field. Particularly, such a formation region effect was observed in [4] for TR in the millimeter wavelength region emitted by electrons with an energy of 150 MeV. A significant suppression of the radiation spectral-angular density, compared to the case of the upstream target absence (when TR is generated by the impinging electron having the conventional unsuppressed Coulomb field), has been observed in this experiment. The analogous effects of radiation suppression due to the "half-bare" state of electrons within the formation region have been studied both theoretically and experimentally for bremsstrahlung [5–10], diffraction radiation [11], as well as (only theoretically) for the coherent x-ray emission in crystals [12–13].

In the present work we experimentally investigate the manifestation of the formation region effects (or the electron "half-bare" state) in the

* Corresponding author at: National Science Center "Kharkiv Institute of Physics and Technology", Akademichna st., 1., Kharkiv 61108, Ukraine.
E-mail address: trofymenko@kipt.kharkov.ua (S.V. Trofymenko).

https://doi.org/10.1016/j.nimb.2020.04.033
Received 22 February 2020; Received in revised form 3 April 2020; Accepted 23 April 2020
Available online 14 May 2020
0168-583X/

spectra of x-ray transition radiation, generated in periodical radiators by electrons in the energy range between 1 and 6 GeV. The radiation of this kind (as well as the analogous emission in the optical range [14]) is of high interest as a source of x-rays [15–18] and a tool for ultra-relativistic particle detection (see, e.g. [19,20]). The comprehensive study of such radiation effects is therefore quite important.

In a multilayer target (radiator), consisting of thin foils separated by short air gaps, the electron "undressing" by an upstream foil and subsequent emission of the TR at the electron incidence on the next downstream foil (the process similar to the one considered in [4]) are repeated many times. We have been using two radiators of sufficiently different period in our experiments. In the large-period radiator (L radiator) the electron has enough time to recover the x-ray Fourier components of its proper field in the gap between the foils. In this case the formation region effects are almost insignificant for the TR spectrum. In the small-period radiator (S radiator) the electron is still considerably "half-bare" at the moments of its impinging upon each next foil (in the result of penetration through each previous one) and the effects discussed above play a significant role. The evolution of the difference between the TR spectra in these radiators with the increase of the electron energy has been studied. Such an evolution reflects the γ dependence of the formation length.

It should be pointed out that in [21] the dependence of TR yield on the radiator period (precisely, on separation between the foils) was studied and suppression of the yield for periods smaller than the TR formation length was observed. However, the effect was investigated only for the total x-ray TR yield (angle and frequency integrated) and the study was performed for a single value of the electron energy (15 GeV).

The main aim of our work was to study the formation region effect for the radiation spectrum (just partially angle-integrated) in the wide range of the radiator period to l_F ratio. For this the radiators of considerably different periods were applied and the electron energy was noticeably varied. Such an approach provided a possibility to observe not only the expected TR suppression in the S radiator (compared to the L radiator), but also the opposite effect of some enhancement of the TR in the S radiator. Previously such an effect had been discussed only theoretically [22] and was not observed under the measurement conditions in [21]. Nonetheless, in our experiment the above enhancement was much smaller than could be expected from the theory of single-particle emission [15] and lay on the verge of statistical uncertainty. Our theoretical estimations indicate that the reason for this was a rather large transversal size of the electron beam (around 5 mm) and the discussed effect should be much more significant for the electron beams of smaller transversal size. The estimations also show that in this case the discussed effect remains rather large even if the registered number of TR photons is integrated with respect to a relatively large range of photon energies (i. e., 10–30 keV). On the basis of these results it is proposed to apply this effect to increase the number of TR photons in a multilayer target, which is used as a source of a highly collimated photon beam.

2. Experiment

The experimental study was performed at DESY II test beam facility in Hamburg using beamline TB21. The facility provides an electron beam with the energy E from 1 to 6 GeV, which is defined by the magnetic field strength in the primary dipole magnet [23]. The layout of the experiment at the test beamline is presented in Fig. 1.

The electron beam was shaped by the vertical and horizontal primary collimators, then passed through a lead collimator of 300 mm length with 5×5 mm^2 square hole and interacted with the L or S radiator. Both primary collimators consist of two tungsten jaws with a length of 100 mm each. The radiators consisted of 50 aluminum foils with a thickness $l_A = 13$ μm separated by air gaps. The period of the L radiator with the total length of 150 mm was 3.0 mm, while the one of S radiator with the total length of 15 mm was 0.30 mm. The total thickness of the aluminum foils is around 0.7% of the total radiation length in both radiators. The surface of the foils was sufficiently smooth and straight and did not contain any visible roughness. After crossing a radiator and generating TR photons the electron beam was deflected using a bending magnet which provided the maximum field strength of 1.35 T. The photon beam arrived at CdTe cooled x-ray detector XR100T [24] with a crystal thickness 1 mm and a square active area 5×5 mm^2. The detection efficiency was close to 100% in the x-ray energy range between 5 and almost 100 keV. The distance from the collimator to the detector amounted to 3720 mm. The detector signal was processed by the digital pulse processor PX5 with the peaking time 2.8 μs. The energy calibration of the spectrometer was performed using x-ray lines from an ^{241}Am source (see Fig. 2). The energy resolution of the spectrometer was measured to be about 0.7 keV at 59.54 keV.

The separate measurements of the electron beam current were performed with a spectrometer measuring the ionization loss of the incident particles. The spectrometer consists of the Si surface-barrier square detector Hamamatsu S3590-18 of the size 10×10 mm^2 and 300 μm thickness of the depleted layer at the bias voltage of 100 Volts [25], a preamplifier A250CF CoolFET [24], and a digital pulse processor PX5 [24] with a peaking time of 0.8 μs. The energy calibration of the spectrometer was made using the x-ray lines from an ^{241}Am source.

The silicon detector was installed in the electron beam at a distance of 3210 mm from the lead collimator and the measurements were performed using electron beam energies in the range 1–6 GeV without any radiators and with the bending magnet switched off. The typical ionization loss spectrum measured at an electron energy of 4 GeV is shown in Fig. 3 (without the background subtraction). It displays the well-known Landau spectral peak for the ionization loss with a most probable energy of the ionization loss of $\Delta_{MP} = 85.5$ keV, which, as expected for any ultrarelativistic particle with a unit charge, is almost the same as in [25] for the case of 50 GeV proton beam crossing the same detector. The number of particles which have passed through the detector was determined by the integration of the number of counts in the Landau peak. The typical electron current was about 750–3400 particles per second in our experiments. The maximum current corresponds to electron energies E between 2 and 3 GeV while its minimum values were on the edges of the electron energy range. The average beam current was found to be stable enough at a fixed electron beam energy in the range 1–6 GeV within a period of time of about few hours. Namely, its variation did not exceed about 2% of its magnitude.

The study of the x-ray spectra consisted of a series of measurements at the electron energies $E = 1.0$, 2.6, 4.0 and 6.0 GeV. For each electron energy three measurements were performed: at first, the L radiator was used, then it was replaced by the S radiator, and finally, the measurement of the background radiation in the absence of radiators was performed. In each measurement the radiation spectrum was being collected during a fixed interval of 30 min, which was possible due to the described above good stability of the electron beam current at each value of the electron energy.

An example of "raw" spectra measured at an electron energy of 4 GeV is presented in Fig. 4. The x-ray radiation spectra for both radiators have wide spectral peaks of transition radiation at the photon energy of around 17 keV. The background spectrum is associated with electromagnetic radiation which accompanies the incident electron beam and is measured without any radiator. The background radiation arises mainly due to bremsstrahlung from both collimators and synchrotron radiation from both magnets (the primary dipole magnet, defining the electron energy, and the bending magnet). Besides, the background spectrum contains additional spectral peaks, representing $K_{\alpha 1}$ (59.318 keV), $K_{\alpha 2}$ (57.982 keV), $K_{\beta 1}$ (67.244 keV) and $K_{\beta 2}$

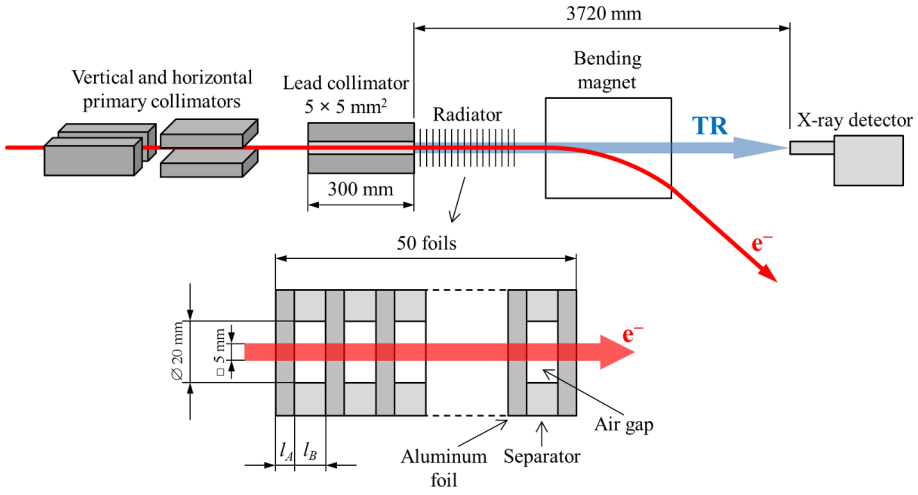

Fig. 1. Schemes of the experimental layout and radiators.

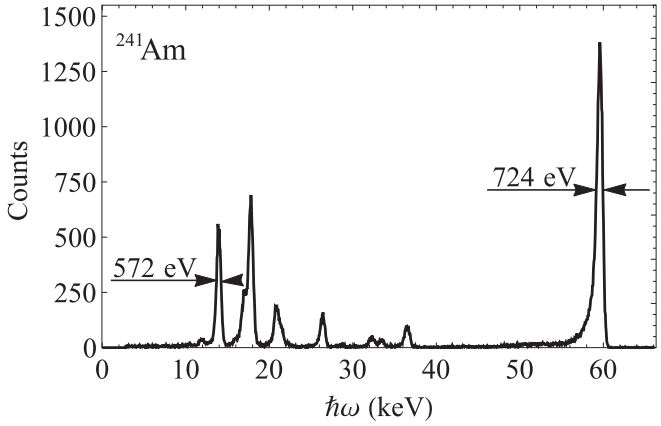

Fig. 2. Calibration x-ray spectrum of an ^{241}Am source measured using an Amptek CdTe detector.

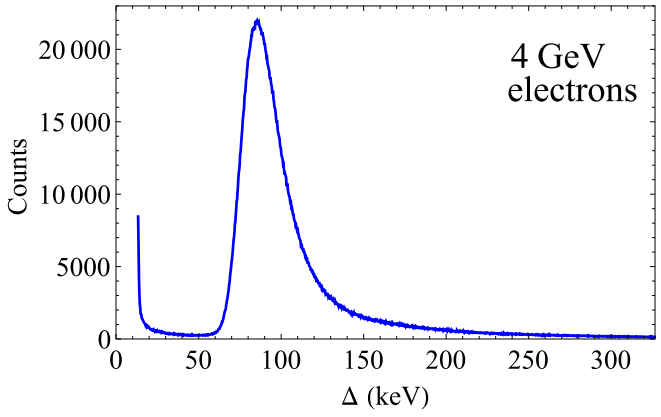

Fig. 3. The spectrum of ionization loss of 4 GeV electrons measured by the Si detector, which contains the Landau spectral peak.

(69.100 keV) lines of the characteristic x-ray radiation of tungsten, which is excited in the jaws of the primary collimators. The background radiation makes its contribution to the spectra measured in the presence of the radiators. In the region of photon energies below 10 keV the radiation significantly attenuates in the air on its way from the radiator to the detector. The energy resolution was controlled using the $K_{\alpha 1}$ spectral peak of tungsten during the experiments and was about

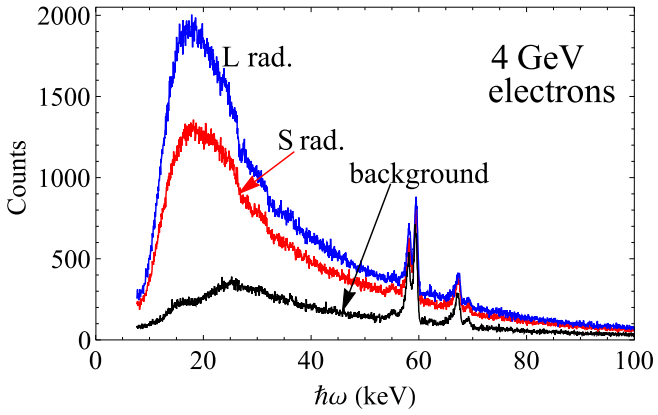

Fig. 4. An example of "raw" x-ray spectra delivered by the spectrometer in the case of 4 GeV electron beam. The curves correspond to separate measurements with the use of L and S radiators, as well as to the measurement of the background radiation in the absence of radiators.

0.7 keV, which is in agreement with the resolution measured using the ^{241}Am source.

3. Theoretical estimations

According to our estimations, the spectral density of the bremsstrahlung generated by the electrons in the foils of the radiators is much smaller than the one of TR in the presently studied range of photon energies. Therefore, it is the TR mechanism of the photon emission which we will consider as the main origin of the wide spectral peak in our theoretical analysis of the measured spectra.

In order to compare the results of measurements with the theoretical predictions it is necessary to make a certain elaboration of the existing formulae describing TR from multilayer targets, in order to make them more adequately corresponding to the conditions of our measurements. This particularly includes the averaging of the TR spectrum with respect to the transversal size of the electron beam, taking into account the finite size of the detector. First, let us discuss the TR spectrum generated by a single electron, outlining the role of the formation length in it.

3.1. Single-electron spectrum

Our consideration is based on the expression, derived in [15]. It defines the spectral-angular density of TR generated by a particle

normally traversing a set of n parallel foils of thickness l_A with the plasma frequency ω_{pA} separated by the gaps of thickness l_B with a plasma frequency ω_{pB}. For a large value of n a simplified formula for the factor describing the interference of contributions from the different foils is presented in [15] as well (formula 3.58). Substituting this formula into the aforementioned expression for the TR spectral-angular density and integrating the latter with respect to observation angles, it is possible to present the expression for the radiation spectrum in the following form:

$$\frac{dN}{d\omega} = n_{eff}(\omega)\frac{8\alpha}{\omega}\frac{(\omega_{pA}^2-\omega_{pB}^2)^2}{\omega^4}\frac{2\mathrm{v}}{\omega l} \times \sum_{k=k_{\min}}^{k_{\max}} \frac{\vartheta_k^2 \sin^2[\omega l_A(\gamma^{-2}+\vartheta_k^2+\omega_{pA}^2/\omega^2)/4\mathrm{v}]}{(\gamma^{-2}+\vartheta_k^2+\omega_{pA}^2/\omega^2)^2(\gamma^{-2}+\vartheta_k^2+\omega_{pB}^2/\omega^2)^2} \tag{1}$$

It is analogous to the corresponding expression derived in [16,21]. However, here we present it in the form which better illustrates the effect of the formation region upon the radiation spectrum (see the considerations below). Here N stands for the number of photons and $n_{eff}(\omega) = (1-e^{-N\sigma})/(1-e^{-\sigma})$ is the effective number of foils which contribute to the spectrum (due to radiation attenuation in the foils). Presently $\sigma = \mu_A l_A$ with μ_A being the foil x-ray attenuation coefficient. The quantity $l = l_A + l_B$ is the radiator period. We also use the following denominations

$$\vartheta_k^2 = \frac{4\pi kc}{\omega l} - \gamma^{-2} - \frac{\langle\omega_p^2\rangle}{\omega^2},\ \langle\omega_p^2\rangle = \frac{\omega_{pA}^2 l_A + \omega_{pB}^2 l_B}{l_A + l_B} \tag{2}$$

$$k_{\min} = \mathrm{Int}\left\{\frac{1}{2\pi}\left(\frac{l_A}{l_{FA}(0)} + \frac{l_B}{l_{FB}(0)}\right)\right\} + 1,$$
$$k_{\max} = \mathrm{Int}\left\{\frac{1}{2\pi}\left(\frac{l_A}{l_{FA}(\vartheta_{\max})} + \frac{l_B}{l_{FB}(\vartheta_{\max})}\right)\right\} \tag{3}$$

as well as

$$l_{FA,B}(\vartheta) = 2\mathrm{v}\omega^{-1}/(\gamma^{-2} + \vartheta^2 + \omega_{pA,B}^2/\omega^2) \tag{4}$$

for the formation length in aluminum foils (A) and air gaps (B) between them. The latter expression accounts for the formation length dependence on the observation angle ϑ (counted from the direction of the particle velocity vector $\vec{v}$) and the plasma frequency of the medium, as well as on the particle Lorentz-factor γ. Formulas (3) follow from the expression for k, directly obtained from (2): $k = \omega l(\vartheta_k^2 + \gamma^{-2} + \langle\omega_p^2\rangle/\omega^2)/(4\pi c)$ with $k_{\min}$ and $k_{\max}$ corresponding to the values of ϑ_k equal to 0 and $\vartheta_{\max}$ respectively. The denomination "Int" in (3) stands for the integer part of the expressions in braces. The values $\vartheta = \vartheta_k$ correspond to the angular positions of the peaks (which, however, have some angular width) in which the major part of the radiated energy is concentrated due to interference of contributions from the separate foils of the radiator. Presently $\vartheta_{\max} = R/L$ is the maximum value of the observation angle (see Fig. 5), defined by the detector radius R and its separation L from the radiator (for simplicity, we assume that the particle moves along the axis which crosses the center of the circular active area of the detector). In our case $l_A/l_B >> \omega_{pB}^2/\omega_{pA}^2$ and the second formula in (2) can be presented as $\langle\omega_p^2\rangle \approx \omega_{pA}^2 l_A/l$. Let us note that expression (1) in a different representation (summation not with respect to the observation angles ϑ_k but with respect to the TR frequencies corresponding to these angles) was obtained in [18]. For the detailed discussion of expression (1) and its experimental verification see [16,21] as well. Also, for accurate angular distributions of TR in multilayer targets and their comparison with the results of GEANT4 simulations see [26].

The values of ϑ_k in (1) cover the same region $(0, \vartheta_{\max})$ irrespective of the radiator period. The only difference between the cases of the L and S radiators (except the quantity l^{-1} in the factor in front of the sum) is associated with the different values of the ratios $l_B/l_{FB}(0)$ and $l_B/l_{FB}(\vartheta_{\max})$ in (3) for these radiators. These ratios involve the formation length values at the borders of the angular region $0 < \vartheta < \vartheta_{\max}$ and define the number of summands in (1). Thus, the difference between the TR spectra generated in L and S radiators is attributed to the different values of both $l_{FB}(0)$ and $l_{FB}(\vartheta_{\max})$ in these radiators. In this sense such a difference of the spectra is presently considered as a formation region effect.

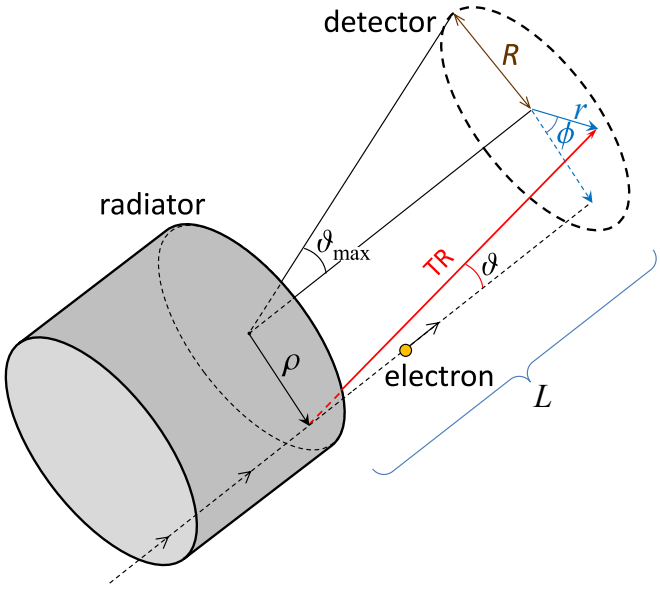

Fig. 5. Scheme of the layout used for calculations.

3.2. Averaging over the transversal size of the beam

In order make a comparison with the experimental results it is necessary to average the expression (1) with respect to the transversal size of the electron beam. It is, however, more convenient to perform such a procedure based on the initial formula for the TR spectral-angular density $N_{\omega,\vartheta}$ from [15]. As previously, we consider the case of a circular detector of radius R first. In this case the averaged value of the TR spectral density (per a single particle of the beam) reads:

$$\left\langle\frac{dN}{d\omega}\right\rangle_{circ} = \frac{2\pi}{L^2}\int_0^R rdr\int_0^{2\pi} d\phi\int_0^{\infty}\rho f(\rho)N_{\omega,\vartheta}d\rho \tag{5}$$

Here r and ϕ are the polar coordinates on the detector surface (see Fig. 5) and ρ is the distance from the particle to the beam axis (which crosses the center of the detector). The function $f(\rho)$, which is normalized to unity, describes the transversal particle distribution of the beam. It is necessary to put $\vartheta = \sqrt{r^2+\rho^2-2r\rho\cos\phi}/L$ in the expression for $N_{\omega,\vartheta}$ in (5) in order to express ϑ via integration variables. Calculating the integrals with respect to r and ϕ in (5), we finally obtain:

$$\left\langle\frac{dN}{d\omega}\right\rangle_{circ} = \frac{32\alpha\pi c N_{eff}(\omega)}{\omega^2 l}\frac{(\omega_{pA}^2-\omega_{pB}^2)^2}{\omega^4}\int_0^{\infty} d\rho\rho f(\rho)\times \tag{6}$$
$$\times\sum_{k=k_{\min}}^{k^+(R,\rho)} g_k\left\{\eta(R-\rho)\eta(k^-(\rho)-k) + \frac{1}{\pi}\arccos\left(\frac{\rho^2+L^2\vartheta_k^2-R^2}{2\rho L\vartheta_k}\right)\eta(k - k^-(\rho))\right\}$$

where

$$g_k = \frac{\vartheta_k^2\sin^2[\omega l_A(\gamma^{-2}+\vartheta_k^2+\omega_{pA}^2/\omega^2)/4c]}{(\gamma^{-2}+\vartheta_k^2+\omega_{pA}^2/\omega^2)^2(\gamma^{-2}+\vartheta_k^2+\omega_{pB}^2/\omega^2)^2},$$
$$k^{\pm}(R,\rho) = \frac{\omega l}{4\pi c}\left(\left(\frac{\rho\pm R}{L}\right)^2 + \gamma^{-2} + \frac{\langle\omega_p^2\rangle}{\omega^2}\right)$$

and $\eta(x)$ is the Heaviside step-function. Like in (1), it is necessary to take the integer part of k^+ in (6), however, it is not the case for k^- which is generally not an integer. The arccos factor in (6) originates from the fact that the "rings", corresponding to the TR angular distribution peaks at $\vartheta = \vartheta_k$ (for each single particle), generally, just partially overlap with the detector surface.

In our experiment the detector surface was square-shaped. In this case, in order to obtain the expression for the averaged radiation spectrum, it is necessary just to add the expression, accounting for the area in the vicinity of the vertices of the square (the side of the square is $2R$), to (6):

$$\left\langle \frac{dN}{d\omega} \right\rangle_{sq} = \left\langle \frac{dN}{d\omega} \right\rangle_{circ} + \left\langle \frac{dN}{d\omega} \right\rangle_{vert} \tag{7}$$

where

$$\left\langle \frac{dN}{d\omega} \right\rangle_{vert} = \frac{8}{\pi} \frac{32\alpha c N_{eff}(\omega)}{\omega^2 l} \frac{(\omega_{pA}^2 - \omega_{pB}^2)^2}{\omega^4} \sum_{k=k_{\min}}^{\infty} g_k \int_0^{\infty} d\rho \rho f(\rho) \times \tag{8}$$

$$\times \int_R^{\sqrt{2}R} dr r \frac{\arcsin((R - \sqrt{r^2 - R^2}) / \sqrt{2} r)}{\sqrt{4r^2\rho^2 - (r^2 + \rho^2 - L^2\vartheta_k^2)^2}}$$
$$\eta(k - k^-(r, \rho))\eta(k^+(r, \rho) - k)$$

For the numerical estimations we take $f(\rho)$ in a Gaussian form as

$$f(\rho) = e^{-\rho^2/2d^2}/2\pi d^2$$

where d is related to the beam full width at half maximum (FWHM) D as $D = d\sqrt{8 \ln 2}$. We take $D = 2R = 0.5$ cm, which corresponds to the size of the collimator exit window. Such a choice of an axially symmetric function $f(\rho)$ is associated with a certain simplification since in our case the collimator exit window has a square shape.

4. Results and discussion

Fig. 6 shows the results of the experimental measurements of the TR spectra generated in the L and S radiators by electrons with energies of 1.0, 2.6, 4.0 and 6.0 GeV. For each energy value the presented spectra are obtained via subtraction of the corresponding background radiation spectrum (in the absence of radiators) from the ones registered in the presence of the radiators (see Fig. 1). It was taken into account that the registered background undergoes an additional attenuation in the foils of the radiators. Due to a relatively low current of the electron beam and significant increase of the background radiation intensity at $E = 6$ GeV, which resulted in rather low statistics, the results of measurements in this case were averaged with respect to three channels of the spectrometer, which corresponds to the increase of the energy interval per channel from 55 eV to 165 eV.

The solid lines demonstrate the results of the corresponding theoretical estimations on the basis of (7). Additional radiation attenuation in the air in the region between the radiator and the detector was taken into account in this case. The results of estimation were normalized in such way that the heights of the maxima of the curves (thick blue) depicting the spectra from the L radiator coincided with the experimental data. This corresponded to multiplication of the calculated radiation spectral density by a factor close to ½ (the same factor was applied both for L and S radiators). The point is that the result of the theoretical estimation of the absolute value of the photon yield exceeded the experimentally measured value by about a factor of two for all values of incident electron energy. We associate this discrepancy with the influence of the electron beam divergence, which expression (7) does not take into account (it is both the initial divergence of the incident electron beam and the additional divergence due to multiple scattering of the electrons in the foils). A rough estimation, based on

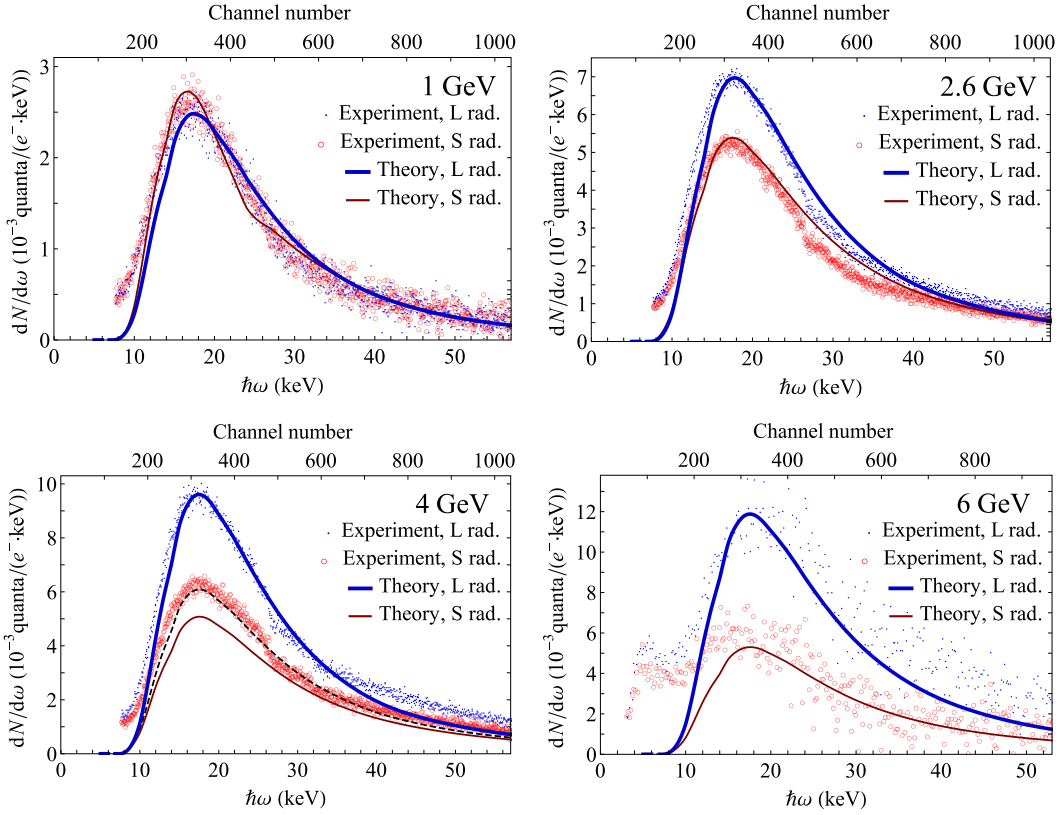

Fig. 6. Spectra of TR from radiators of different period for various electron energies E (with subtracted spectra of background radiation). Blue points – the experimental results for L radiator ($l = 3.0$ mm), red circles – the analogous results for S radiator ($l = 0.3$ mm). Thick solid blue line – the theoretical estimation for L radiator, thin solid red line – the analogous estimation for S radiator. Dashed line in the figure depicting the $E = 4$ GeV case shows the theoretical estimation of the spectrum for the size of the gap between the foils $l_B = 0.4$ mm.

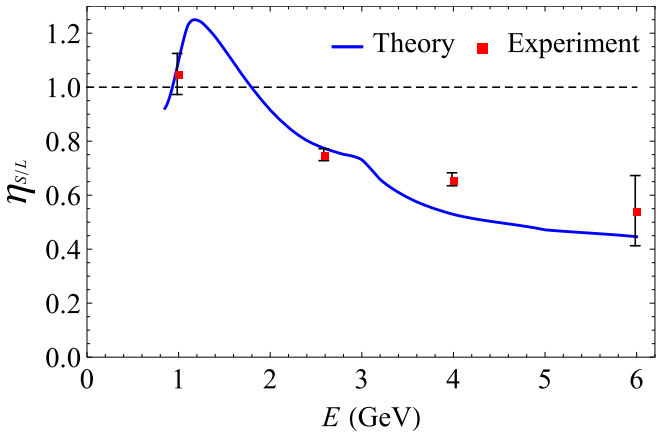

Fig. 7. Dependence of the ratio of the TR spectral density (at the maxima of the spectra) in the S radiator to the one in the L radiator on the incident electron energy.

pure geometrical considerations, indicates that, due to such a divergence, the photon flux through the detector under conditions of our experiment is almost half as much compared to the case of an ideally parallel beam. Note that the similar exceeding of the measured intensity by the calculated data was also indicated in a series of previous works (see [21], as well as [27] and refs. therein) both for the TR spectral density and total yield. Such a discrepancy, observed in the previous and present works, seems to be worthy of further study. Also note that presently we did not observe the spectrum oscillations originating from the single-foil interference, described by the sine squared factor in (1), since in our case they belong to the region of photon energies less than 10 keV and are completely suppressed by TR absorption in the air.

The energy of the wide asymmetrical spectral peak at about 17 keV is almost independent on the incident electron beam energy and is in good agreement for the calculated and measured spectra. In spite of the above discrepancy in the absolute values of the calculated and measured spectral densities by about a factor of 2, the shapes of the measured and calculated spectra, shown in Fig. 6, agree quite well at photon energies exceeding 10 keV for both L and S radiators. This leads to the conclusions that the observed difference of the spectra from the L and S radiators can be attributed to the formation region effect, as predicted by the theory. For $E = 4$ GeV, however, the theory predicts a lower value of the TR intensity from the S radiator at the maximum of the spectrum than the experimentally observed one. This might be attributed to the fact that in the course of the corresponding measurement the bracing, which squeezed the rings in the S radiator, has slightly weakened, which resulted in the increase of the gaps between the foils (the bracing was fixed again before further measurements). It is supported by the fact that the calculation for a slightly larger value of l (namely, $l = l_A + l_B \approx 0.4$ mm), depicted by the dashed line in the corresponding figure, demonstrates a much better coincidence with the experimental data.

The radiation in all the measured spectra at the values of photon energy below about 10 keV is not described by our calculations based on the transition radiation mechanism, which predict a zero yield in this energy range predominantly as a result of TR attenuation in the foils and in the air. The origin of this radiation is not clear so far, but it is not due to the background synchrotron or bremsstrahlung radiation accompanying the incident electron beam, since such a background is subtracted. Hence, the prime candidate is scattering of the electrons in the foils of the radiators. For instance, a part of the particles, scattered in the radiator in the direction opposite to the one of the subsequent deflection, can produce a more intensive synchrotron radiation in the bending magnet, which then hits the detector. Such radiation is obviously absent in the background spectra and therefore could not be subtracted. The synchrotron radiation is less attenuated in the air than TR since the bending magnet is nearer to the detector than the radiator. Anyway, the clarification of the origin of the radiation with the energy below the wide spectral TR peak will require additional investigations.

In general, Fig. 6 demonstrates a distinct suppression of the TR spectrum from the S radiator compared to the one from the L radiator for the electron energies 2.6, 4.0 and 6.0 GeV. The relative magnitude of the suppression grows with the increase of the electron energy, which reflects the proportional increase of the formation length. Let us, for illustration, take the value $\vartheta = 0$ for the observation angle and $\hbar\omega = 17$ keV for the photon energy in (4), which approximately corresponds to the maxima of the observed spectra. In this case for the L radiator the value of l_B/l_{FB} at the electron energies 1.0, 2.6, 4.0 and 6.0 GeV is 34.14, 5.25, 2.35 and 1.17. Hence, in such a radiator the electron has enough time to recover its Coulomb field up to the moment of impinging upon each next foil after being "undressed" in the result of crossing the previous foil. In this case the spectrum is almost not influenced by the formation region effect and is close to the spectrum which takes place in the absence of any interference between the emissions of separate foils. For the S radiator, on the contrary, the corresponding values of l_B/l_{FB} for $E = 2.6$, 4.0 and 6.0 GeV are 0.52, 0.23 and 0.12, which is significantly less than unity. This results in the observed suppression of the radiation intensity.

At $E = 1$ GeV the intensity of TR from the S radiator at the maximum of the spectrum slightly exceeds the corresponding intensity from the L radiator, which is the effect opposite to the one taking place at higher values of E. In the present case the value of l_B/l_{FB} for the S radiator, estimated for the same ϑ and ω as before, is 3.37. In this case the spectrum in the S radiator is almost the same as in the L one. However, the slight constructive interference between the emissions of separate foils is manifested in this case. It leads to a small enhancement of the TR intensity. Such an effect of TR intensity enhancement compared to its value at $l_B >> l_{FB}$, which can be manifested at $l_B \sim l_{FB}$, is discussed in more detail in Sec. 5. The analogous effect of small radiation enhancement for the case of electron bremsstrahlung in the gamma range in a system of two targets was studied previously both experimentally [28] and theoretically (see [29] and refs. therein).

Fig. 7 summarizes the main points, concerning the influence of the formation region effects upon the TR spectrum, discussed above. It depicts the ratio $\eta_{S/L}$ of the TR spectral density in the S radiator to the one in the L radiator as a function of the incident electron energy. The theoretical values of the intensity (solid line) are calculated here at the maxima of the spectra. The experimental points are obtained via averaging of the data in the narrow region of the width $\Delta\hbar\omega \approx 1$ keV around the energies corresponding to the maxima of the spectra. Here we see that the enhancement of the radiation intensity in the S radiator compared to the radiation intensity in the L one, observed for $E = 1$ GeV, is expected to be more significant for $E \approx 1.2$ GeV. The discrepancy between the theory and the experiment for $E = 4$ GeV was discussed above. The analogous discrepancy for $E = 6$ GeV can be attributed to low statistics and influence of the synchrotron radiation (which should be more intense at this energy compared to the lower ones) produced in the bending magnet by the electrons scattered in the radiator, which could not be subtracted, as we mentioned above.

5. On the optimal l_B value for TR generation at small ϑ_{max}

It is necessary to note that under certain conditions the mentioned effect of radiation intensity enhancement, compared to its asymptotic value at $l_B >> l_{FB}$, which was rather small in our experiment, can be quite significant for the TR yield (even if it is integrated with respect to angles and frequency), provided the acceptance angle ϑ_{max} is rather small. Estimations for different values of ϑ_{max} indicate that such an effect is most noticeable for $\vartheta_{max} \sim 1/\gamma$. The value of l_B, corresponding to the largest magnitude of the yield, can be estimated from the following qualitative reasoning. The values of $\vartheta = \vartheta_k$, which are defining the

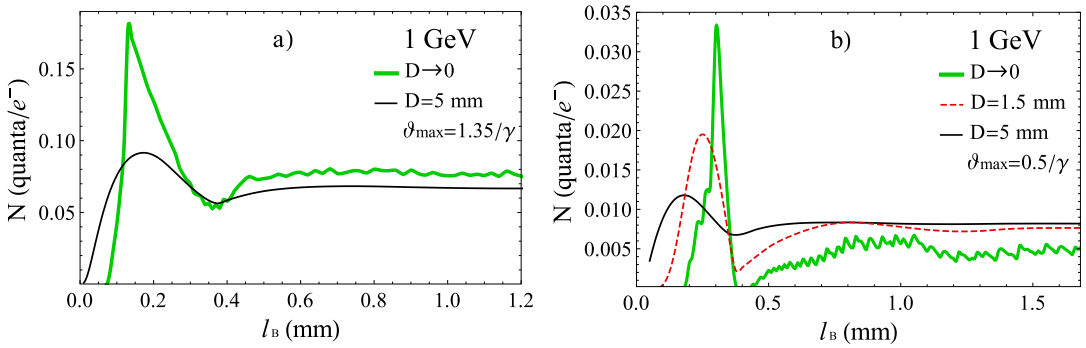

Fig. 8. Dependence of the TR yield in the region of photon energies 10–30 keV on l_B for two values of the detector acceptance angle ϑ_{max}. The lines correspond to different values of D, which is the electron beam transversal size (FWHM).

angular positions of the peaks where the major part of the radiated energy is concentrated, decrease with the increase of l_B, according to (2). A sudden increase of the yield with the increase of l_B (for $l_B \sim l_{FB}$) can be attributed to the "entrance" of the values ϑ_k into the region $(0, \vartheta_{max})$. For a given frequency ω it is natural to expect a maximum in the yield (as a function of l_B) each time when a value of ϑ_k (for each next k) becomes less than ϑ_{max}. In fact, it turns out that for the electron energy range, discussed in the present paper, the maximum in the yield is most noticeable only for $k = 1$. The entrance of the higher order peaks into the detector acceptance region just results in the gradual establishment of the asymptotic value of the yield, corresponding to $l_B >> l_{FB}$ (the number of the peaks in the region $(0, \vartheta_{max})$ increases with a simultaneous decrease of single peak contributions). Putting $\vartheta_k = \vartheta_{max}$ together with $k = 1$ in (2), it is possible to estimate the value l_B^m of l_B corresponding to the yield maximum as

$$l_B^m \approx \frac{4\pi c/\omega - \omega_{pA}^2 l_A/\omega^2}{\vartheta_{max}^2 + \gamma^{-2}} \tag{9}$$

where we applied the relations $\langle\omega_p^2\rangle \approx \omega_{pA}^2 l_A/l$ and $l \approx l_B$ as well. If the yield is considered in a certain frequency range, the quantity ω in (9) should be treated as some typical frequency of the spectrum, e. g., the one corresponding to its maximum, provided there is a maximum within the considered range. Expression (9) describes rather well the maximum position up to electron energies of about 7 GeV for $\vartheta_{max} \leqslant 2/\gamma$. At higher energies formula (9) gives an overestimated value for l_B^m. Additional maxima (associated with $k = 2, 3, \ldots$) also appear in the dependence of the yield on l_B in this case (provided $\vartheta_{max} \sim 1/\gamma$).

Fig. 8a shows an example of the TR yield dependence on l_B for the conditions typical for our experiment ($E = 1$ GeV, $\vartheta_{max} \sim 6.8 \cdot 10^{-4} \approx 1.35/\gamma$). The yield is integrated with respect to the region of photon energies between 10 and 30 keV. Presently we do not take into account the absorption in the air on the way to the detector when estimating the number of emitted photons. The solid green line depicts the result of estimation on the basis of (1), valid for a beam with a negligibly small transversal size (much smaller than the one of the detector). It indicates that a noticeable enhancement (by about a factor of two) of the radiation intensity, compared to its asymptotic value at $l_B >> l_{FB}$, takes place in this case. Presently expression (9) gives the value $l_B^m \approx 0.134$ mm for the separation l_B between the foils at the maximum of the yield (for keV, approximately corresponding to the maximum of the spectrum in the absence of the photon absorption in the air), which nicely coincides with the maximum position in the figure. The formation distance in this case (for the same ω and $\vartheta = 0$) is $l_{FB} \approx 0.1$ mm and, as expected, is of the same order of magnitude as l_B^m.

The thin black line in Fig. 8a corresponds to the yield averaged with respect to the transversal size of the beam for the value $D = 0.5$ cm, which was applied in Sec. 4 (for the case of a square detector, as in the experiment). It shows that such averaging decreases the yield in the maximum, which was the reason of a rather small magnitude of the effect of the TR intensity enhancement in the S radiator in our experiment (Fig. 6, the case of 1 GeV). Thus, the beams of sufficiently small transversal size (smaller than the size of the detector) are preferable for the discussed effect of radiation enhancement to be manifested.

The effect of enhancement of the radiation yield becomes more significant for smaller values of the acceptance angle ϑ_{max}. For instance, Fig. 8b depicts the results of estimation for $\vartheta_{max} = 0.5/\gamma$. Here we see that in the present case, for a sufficiently thin beam, the intensity in the maximum exceeds the one for $l_B >> l_{FB}$ by about a factor of six. Presently, according to (9), $l_B^m \approx 0.3$ mm. As before, it coincides with the formation length ($l_{FB} \approx 0.1$ mm) by the order of magnitude, however, in this case $l_B^m/l_{FB} \approx 3$. The lines for D = 1.5 mm and D = 5.0 mm in Fig. 8b are obtained with the use of (6) for the case of a circular detector.

Note that in the case $\vartheta_{max} < 1/\gamma$ it might be more practical to place the center of the detector active area in the direction of $\vartheta = 1/\gamma$, not $\vartheta = 0$, to achieve a larger photon yield. The l_B dependence of the yield in this case is analogous to the one depicted in Fig. 8 and the formula (9) still defines the position of the sharp maximum.

In general, the discussed figures show that in the case of the detector acceptance angles $\vartheta_{max} \sim 1/\gamma$ there is a preferable value l_B^m of separation between the foils. By choosing this optimal separation, it is possible to noticeably increase the number of emitted TR photons compared to emission in the analogous stack acting as a set of independent foils (as in the case $l_B >> l_{FB}$). These results may be of interest for the application of multilayer targets as sources of narrowly collimated photon beams. Besides, the ratio of the yield values at $l_B = l_B^m$ and $l_B >> l_{FB}$ depends on D (see Fig. 8b), which could be used for the estimation of the beam transversal size.

The possibility of the existence of a maximum in the dependence of the photon yield on the spacing between the foils was already indicated in [22]. However, the authors considered the number of TR photons integrated with respect to the whole range of the emission angles (unlike our case of the integration with respect to a small region of these angles). In that case the radiation intensity in the maximum exceeded the asymptotic value of the TR intensity (for a large spacing) by less than 30%.

6. Conclusion

In the present work the manifestation of radiation formation region in the spectral properties of x-ray TR due to multi-GeV electrons in multilayer targets is studied. For this aim the TR spectra generated in the two radiators of different periods were compared. The period of the first radiator (L) exceeded the typical size of the formation length l_F (at a photon energy corresponding to the maximum of the spectra) in the considered process. The period of the second radiator (S) was smaller than l_F, except for the case of the lowest electron energy (1 GeV).

The wide spectral peak of the transition radiation in the energy

range between 10 and 30 keV was observed in the x-ray spectra from both radiators at the electron beam energies 1–6 GeV. The absolute yield of the transition radiation from the both multilayered targets was measured. Suppression of the TR spectrum from the S radiator compared to the one from the L radiator was observed for the electron energies 2.6, 4.0 and 6.0 GeV. The relative magnitude of the suppression increased with the increase of the electron energy, which reflected the simultaneous increase of the formation length.

For $E = 1.0$ GeV the opposite effect, which is a slight enhancement of the TR spectral intensity from the S radiator compared to the one from the L radiator, was observed. It is attributed to manifestation of the constructive interference between the emissions of the individual foils. It is shown that such an effect of radiation intensity enhancement, compared to its asymptotic value at $l_B >> l_{FB}$, achieves a noticeable magnitude for detector acceptance angles in the order of $1/\gamma$. In this case for electron beams of a sufficiently small transversal size it is possible to achieve increase of the radiation yield by several factors due to the proper choice of the separation between the foils. Such an effect could be applied to achieve a noticeable enhancement of the radiation yield in the case when the multilayer target is used as a source of a narrowly collimated photon beam.

For the theoretical estimations expressions for the spectral density of TR from multilayer targets were derived taking into account the averaging with respect to the transversal size of the electron beam. Such expressions are obtained both for detector active areas with a circular and a square shape.

CRediT authorship contribution statement

S.V. Trofymenko: Conceptualization, Investigation, Formal analysis, Writing - original draft. **R.M. Nazhmudinov:** Conceptualization, Methodology, Investigation, Data curation, Software, Visualization. **A.V. Shchagin:** Conceptualization, Methodology, Investigation, Supervision, Writing - original draft. **A.S. Kubankin:** Methodology, Investigation, Validation. **A.P. Potylitsyn:** Methodology, Investigation, Validation. **A.S. Gogolev:** Investigation. **N.A. Filatov:** Investigation. **G. Kube:** Resources. **N.A. Potylitsina-Kube:** Project administration, Funding acquisition. **M. Stanitzki:** Resources, Writing - review & editing. **R. Diener:** Resources. **A. Novokshonov:** Resources.

Declaration of Competing Interest

The authors declare that they have no known competing financial interests or personal relationships that could have appeared to influence the work reported in this paper.

Acknowledgments

The work was partially supported by the project AIDA within the European Union's Horizon 2020 research and innovation program under grant agreement No 654168. The measurements leading to the presented results have been performed at the Test Beam Facility at DESY Hamburg (Germany), a member of the Helmholtz Association (HGF). The work of S. V. T. was partially supported by the project C-2/50-2020 of the National Academy of Sciences of Ukraine (budget program "Support for the Development of Priority Areas of Scientific Research", 6541230). The work of R. M. N., A. V. S. and A. S. K. was financially supported by a Program of the Ministry of Education and Science of the Russian Federation for higher education establishments, project No. FZWG-2020-0032 (2019-1569). The work of A. P. P., A. S. G. and N. A. F. was supported by Tomsk Polytechnic University Competitiveness Enhancement Program.

References

[1] V.L. Ginzburg, V.N. Tsytovich, Transition Radiation and Transition Scattering, Adam Hilger, Bristol, 1984.
[2] P. Rullhusen, X. Artru, P. Dhez, Novel Radiation Sources using Relativistic Electrons: From Infrared to x-rays, World Scientific, Singapore, 1998.
[3] E. L. Feinberg, Zh. Eksp. Teor. Fiz. 50, 202 (1966) [Sov. Phys. JETP 23, 132 (1966)].
[4] Y. Shibata, K. Ishi, T. Takahashi, T. Kanai, F. Arai, S.I. Kimura, T. Ohsaka, M. Ikezawa, Y. Kondo, R. Kato, S. Urasawa, T. Nakazato, S. Niwano, M. Yoshioka, M. Oyamada, Phys. Rev. E 49 (1994) 785.
[5] L. D. Landau, I. Y. Pomeranchuk, Dokl. Akad. Nauk SSSR 92, 535 (1953) [Collected papers of L. D. Landau, edited by D. Ter Haar, Pergamon Press, Oxford, 1965, pp. 589].
[6] A.B. Migdal, Phys. Rev. 103 (1956) 1811.
[7] F. F. Ternovsky, Zh. Eksp. Teor. Fiz. 39, 171 (1960) [Sov. Phys. JETP 12, 123 (1961)].
[8] N.F. Shul'ga, S.P. Fomin, JETP Lett. 27 (1978) 117.
[9] P.L. Anthony, R. Becker-Szendy, P.E. Bosted, M. Cavalli-Sforza, L.P. Keller, L.A. Kelley, S.R. Klein, G. Niemi, M.L. Perl, L.S. Rochester, J.L. White, Phys. Rev. Lett. 75 (1995) 1949.
[10] H.D. Thomsen, J. Esberg, K. Kirsebom, H. Knudsen, E. Uggerhøj, U.I. Uggerhøj, P. Sona, A. Mangiarotti, T.J. Ketel, A. Dizdar, M.M. Dalton, S. Ballestrero, S.H. Connell, Phys. Lett. B 672 (2009) 323.
[11] G. Naumenko, X. Artru, A. Potylitsyn, Y. Popov, L. Sukhikh, M. Shevelev, J. Phys.: Conf. Ser. 236 (2010) 012004.
[12] S.V. Trofymenko, Phys. Rev. A. 98 (2018) 023813.
[13] S.V. Trofymenko, N.F. Shul'ga, A.V. Shchagin, Phys. Rev. Accel. Beams 22 (2019) 024501.
[14] Y. B. Fainberg, N. A. Khizhnyak, Zh. Eksp. Teor. Fiz. 32, 883 (1957) [Sov. Phys. JETP 5, 720 (1957)].
[15] X. Artru, G.B. Yodh, G. Mennessier, Phys. Rev. D 12 (1975) 1289.
[16] M.L. Cherry, Phys. Rev. D 17 (1978) 2245.
[17] M.A. Piestrup, D.G. Boyers, C.I. Pinkus, G.D. Qiang Li, M.J. Hallewell, D.M. Moran, R.M. Skopik, X.K. Silzer, D.D. Maruyama, Snyder, G.B. Rothbart, Phys. Rev. A 45 (1992) 1183.
[18] V.N. Baier, V.M. Katkov, Nucl. Instrum. Methods Phys. Res., Sect. A 439 (2000) 189.
[19] B. Dolgoshein, Nucl. Instrum. Methods Phys. Res., Sect. A 326 (1993) 434.
[20] X. Lin, S. Easo, Y. Shen, H. Chen, B. Zhang, J.D. Joannopoulos, M. Soljačić, I. Kaminer, Nature Phys. 14 (2018) 816.
[21] M.L. Cherry, G. Hartmann, D. Müller, T.A. Prince, Phys. Rev. D 10 (1974) 3594.
[22] G.M. Garibian, Shi Yan, *X-ray Transition Radiation*, Publ. Acad. Sci. Arm, SSR, Yerevan, 1983 [in Russian].
[23] R. Diener, J. Dreyling-Eschweiler, H. Ehrlichmann, I.M. Gregor, U. Kötz, U. Krämer, N. Meyners, N. Potylitsina-Kube, A. Schütz, P. Schütze, M. Stanitzki, Nucl. Instrum. Methods Phys. Res., Sect. A 922 (2019) 265.
[24] https://www.amptek.com.
[25] R.M. Nazhmudinov, A.S. Kubankin, A.V. Shchagin, N.F. Shul'ga, S.V. Trofymenko, G.I. Britvich, A.A. Durum, M.Yu. Kostin, V.A. Maisheev, Yu.A. Chesnokov, A.A. Yanovich, Nucl. Instrum. Methods Phys. Res., Sect. B 391 (2017) 69.
[26] A.A. Savchenko, D.Yu. Sergeeva, A.A. Tishchenko, M.N. Strikhanov, Phys. Rev. D 99 (2019) 016015.
[27] M.L. Cherry, D. Müller, Phys. Rev. Lett. 38 (1977) 5.
[28] K.K. Andersen, S.L. Andersen, H. Knudsen, R.E. Mikkelsen, H.D. Thomsen, U.I. Uggerhøj, T.N. Wistisen, J. Esberg, P. Sona, A. Mangiarotti, T.J. Ketel, Phys. Lett. B 732 (2014) 309.
[29] M.V. Bondarenco, N. F. Shul'ga, Phys. Rev. D, 90, (2014), 116007; Erratum Phys. Rev. D 95 (2017) 019901.